



## **A dynamic model of maize 3D architecture: application to the parameterisation of the clumpiness of the canopy**

M. España, Frédéric Baret, Michaël Chelle, Franck Ariès, Bruno Andrieu

### **► To cite this version:**

M. España, Frédéric Baret, Michaël Chelle, Franck Ariès, Bruno Andrieu. A dynamic model of maize 3D architecture: application to the parameterisation of the clumpiness of the canopy. *Agronomie*, 1998, 18 (10), pp.609-626. hal-02690554

**HAL Id: hal-02690554**

**<https://hal.inrae.fr/hal-02690554>**

Submitted on 1 Jun 2020

**HAL** is a multi-disciplinary open access archive for the deposit and dissemination of scientific research documents, whether they are published or not. The documents may come from teaching and research institutions in France or abroad, or from public or private research centers.

L'archive ouverte pluridisciplinaire **HAL**, est destinée au dépôt et à la diffusion de documents scientifiques de niveau recherche, publiés ou non, émanant des établissements d'enseignement et de recherche français ou étrangers, des laboratoires publics ou privés.

# A dynamic model of maize 3D architecture: application to the parameterisation of the clumpiness of the canopy

Maria España<sup>a</sup>, Frédéric Baret<sup>a\*</sup>, Michael Chelle<sup>b</sup>, Frank Aries<sup>c</sup>, Bruno Andrieu<sup>b</sup>

<sup>a</sup> Bioclimatologie, Inra, Site Agroparc, 84914 Avignon, France

<sup>b</sup> Bioclimatologie, Inra, 78 850 Thiverval-Grignon, France

<sup>c</sup> Biométrie, Inra, Site Agroparc, 84914 Avignon, France

(Received 20 April 1998; accepted 6 October 1998)

**Abstract** – A dynamic 3D maize canopy architecture model is proposed for radiative transfer computation required for canopy functioning or remote sensing applications. It is based on a previous static model describing the 3D architecture of fully developed plants observed at the male anthesis stage. Laws of development and growth in dimension of the stem and the leaves are established based on experimental observations, in order to infer plant architecture at any stage from that of fully developed plants. The leaf curvature and shape are assumed to be the same over the whole leaf duration, with the exception when leaves are still within the top leafy cone at younger stages. The time is described by the number of visible leaves, which can easily be deduced from the cumulated growth degree days. The model requires only four input variables: the sowing pattern (row distance, plant density), the final number of leaves produced, the maximum height at anthesis, and the cumulated leaf area for the fully developed plants. It was validated on independent data sets and provides globally good performances. The model is later used to parameterise the canopy gap fraction which is one of the main variables governing radiative transfer processes. The gap fraction  $P_0(\theta)$  for the observation direction is classically described by an exponential function of the leaf area index,  $L$ :

$$P_0(\theta) = e^{-\lambda_0 \frac{G(\theta, \theta_f)}{\cos \theta} \cdot L}$$

where  $\lambda_0$  is the clumping parameter describing the non-random leaf arrangement and  $G$  is the projection function that depends on the leaf inclination distribution function. The gap fraction model was adjusted over a time series of maize canopies simulated using our 3D dynamic canopy architecture model. We showed that maize canopies have a marked clumped character, with an average clumping parameter of  $\lambda_0 \approx 0.8$ . However, results suggest that the clumping parameter depends on the developmental stage of the canopy, and, to a lesser degree, on the observation direction  $\theta$ .  
(© Inra/Elsevier, Paris.)

maize canopy / architecture / plant development / leaf area index / gap fraction

---

Communicated by Gérard Guyot (Avignon, France)

---

\*Correspondence and reprints

Tel: (33) (0)4 90 31 61 11; fax: (33) (0)4 90 31 64 20; e-mail: baret@avignon.inra.fr

**Résumé – Un modèle dynamique d'architecture 3D du maïs : application à la description de l'agrégation du couvert.** Un modèle 3D d'architecture de maïs est proposé. Il permet de simuler le transfert radiatif dans le couvert nécessaire à la description du fonctionnement de la végétation, ou aux études de télédétection. Il est basé sur un modèle statique précédent de représentation de l'architecture 3D de plantes de maïs complètement développées (stade de l'épiaison mâle). Des lois de croissance en dimension des feuilles et des tiges ont été établies à partir d'observations expérimentales, de manière à décrire l'architecture des plantes pour tout stade à partir de l'architecture des plantes complètement développées. La courbure et la forme des feuilles sont supposées être les mêmes durant toute la vie de la feuille, sauf au moment où elles apparaissent dans le cornet. Le temps est décrit par le nombre de feuilles apparues, qui peut être facilement déduit de la somme des températures. Le modèle nécessite quatre variables d'entrée: la géométrie du semis (distance entre rangs et entre plantes), le nombre de feuilles produites et la hauteur de la plante à la floraison, ainsi que la surface foliaire totale produite des plantes complètement développées. Le modèle, validé sur des jeux de données indépendants, donne une bonne représentation de la structure 3D du couvert. Ce modèle est ensuite utilisé pour étudier la fraction de trous qui constitue une des variables principales du transfert radiatif. La fraction de trous  $P_0(\theta)$ , observée dans la direction  $\theta$ , est classiquement décrite par une fonction exponentielle de l'indice foliaire,  $L$ :

$$P_0(\theta) = e^{-\lambda_0 \frac{G(\theta, \theta_f)}{\cos \theta} \cdot L}$$

où  $\lambda_0$  est le paramètre d'agrégation décrivant la distribution spatiale non aléatoire des feuilles, et  $G$  est la fonction de projection qui dépend de la distribution des inclinaisons foliaires. La fraction de trous a été ajustée sur une série temporelle de couverts de maïs générée par notre modèle dynamique d'architecture 3D. Les résultats montrent que les couverts de maïs ont un caractère agrégé marqué, avec un paramètre d'agrégation proche de  $\lambda_0 \approx 0.8$ , qui dépend à la fois du stade de la culture et de la direction d'observation. (© Inra/Elsevier, Paris.)

**architecture / structure / couvert maïs / développement / indice foliaire / fraction de trous**

## 1. INTRODUCTION

Canopy architecture influences light absorption and scattering in the vegetation. A realistic description of canopy structure is therefore critical to accurately simulate radiative transfer in the vegetation that is useful for canopy functioning or remote sensing applications.

Canopy architecture, as observed at a given time, results from the dynamic process of plant growth and development which confers high consistency to its evolution pattern. This process may be formalised by dynamic modelling of canopy architecture. Dynamic models have been proposed in the last years. They are either purely empirical or incorporate some knowledge of botanical, phenological and physiological rules governing plant growth and development. De Reffye et al. [31] and Jaeger and de Reffye [20] have developed the AMAP model of plant architecture that is mainly driven by botanical rules. Lewis and Muller [24], and Lewis [23] also developed BPMS, a botanical model of plant description. The Lindermayer systems (L-system)

offer an efficient way for describing complex architectures that allow the incorporation of botanical processes [29, 30]. Although maize has got a rather simple architecture, Goel et al. [19] and Fournier and Andrieu [13, 14] applied the L-system approach to model the dynamics of maize architecture.

Recently, a model describing the shape, curvature, dimensions and height of leaves of fully developed maize plants has been proposed by España [11]. It allows the computation of very realistic 3D maize plants. The only input variables of this model are the number of leaves produced by the plant, its total leaf area, and plant height. The simulated plants are used to generate maize canopies according to plant density and sowing pattern. However, because the validity of this model is restricted to fully developed static maize plants, we propose here to extend its domain of validity to the period from emergence to male anthesis. This is achieved by incorporating rules of development that describe the architecture over the whole vegetative growing season.

Our dynamic model will consist in interpolating canopy architecture from an initial stage up to the fully-developed plant as described by España [11]. We will therefore first describe this extension of the original static 3D maize architecture model. The model will then be calibrated with a first experimental data set, mainly focusing on structural variables, and evaluated with independent data sets by comparing experimental and simulated canopy characteristics.

Special attention is paid to the gap fraction, which is one of the main variables used in radiative transfer modelling [1, 4]. The gap fraction  $P_0(\theta)$  for a given canopy structure can be related to its leaf area index ( $L$ ) through a theoretical model [26]:

$$P_0(\theta) = e^{-K(\theta) \cdot L} \quad (1)$$

where  $K(\theta)$  is the extinction coefficient which depends only on the observation direction. When the leaf azimuth distribution is assumed to be random, which is generally the case, the observation direction resumes to the zenith angle ( $\theta$ ). The extinction coefficient is expressed as follows:

$$K(\theta) = \lambda_0 \frac{G(\theta, \theta_1)}{\cos \theta} \quad (2)$$

where the function  $G(\theta, \theta_1)$  is the orthogonal projection of a unit leaf area along direction  $\theta$ . It depends on the leaf inclination distribution, that can be characterised by its average leaf inclination angle  $\theta_1$ . The parameter  $\lambda_1$  is commonly called the leaf dispersion or clumping parameter. Homogeneous randomly distributed leaf canopies are characterised by  $\lambda_0 = 1$ . Clumped canopies for which the leaves overlap preferentially have  $\lambda_0 < 1$ . Conversely, canopies for which the leaves preferentially fill the gaps are termed regular canopies and are characterised by  $\lambda_0 > 1$ . The parameter  $\lambda_0$  characterises the efficiency with which the canopy traps light. The product  $\lambda_0 \cdot L$  may be considered as the effective leaf area index with regards to light interception. This parameter may vary with the observation direction [4] and indirectly with the leaf area index since dense canopies have specific mechanisms to adapt their structure for optimal resource use, including light use. For maize (row canopies) where leaves are obviously clumped around the

stem, the assumption of a random leaf spatial distribution is not valid. We will therefore evaluate the departure of maize canopies from the random assumption using the  $\lambda_0$  parameter.

There are very few theoretical backgrounds describing the clumping effect on radiative transfer [22]. Few studies report experimental values and range of variation of this clumping parameter [1, 27, 33]. In most cases, it is estimated by using either the temporal, spatial or directional variation of the canopies gap fraction using equations (1) and (2) and the measured value of the leaf area index. However, in most cases, assumptions are made about its dependency on the observation direction and the leaf area index. It is used as an indicator of structural changes due to either phenological stages, growth conditions, or variation of vertical profiles within the canopy. In the case of computer generated canopies, the gap fraction may be easily calculated by projecting the simulated canopy onto a plane perpendicular to the direction of observation [5, 6]. In this study, we will use a 3D dynamic architecture model to investigate the range of variation of the  $\lambda_0$  parameter and its sensitivity to the factors described just previously.

## 2. THE MAIZE DYNAMIC 3D ARCHITECTURE MODEL

Our dynamic 3D canopy architecture model is made from a dynamic 3D plant architecture model coupled with a given sowing pattern. We will first present the general principles that drive the plant model development. We will then calibrate the plant model with experimental observations.

### 2.1. Description of the model

We suppose that the canopy is not subjected to brutal stresses or strong mechanical constraints such as that imposed by wind; growth is considered as a smooth process occurring from emergence to male anthesis.

For maize canopies, the phenological stage is measured by the number of leaves produced since emergence that are not totally hidden in the top leafy cone. It may be described using the sum of daily average temperature over a given threshold value [7, 34–36]. The cumulated temperature required between the apparition of two consecutive leaves is approximately constant for a given cultivar and location. The leaf stage used as a measure of time scale presents the advantage of being quite general: it does not require the specification of the sowing or emergence date, the cultivar or location of the canopy, or the temperature regime to which the canopy is subjected.

The static model used for fully developed plants [11] describes the plant dimensions through empirical relationships using three input variables: the final number of leaves produced, the maximum height, and the cumulated leaf area. The shape and curvature of the leaves are described by simple geometrical patterns for which the parameters are randomly drawn within the observed distribution laws.

In the following, we will describe the dynamics of the dimensions, height, senescence, curvature and insertion angle of the leaves, as well as the temporal evolution of the stem dimensions.

### **2.1.1. Evolution of leaf curvature and insertion angle**

Leaves are produced by the apex which is located at the extremity of the stem. They appear first vertically in the top leafy cone, and progressively get their final curvature and insertion angle. We therefore considered three cases:

- the three last leaves that appeared in the top leafy cone are supposed to be sheathed, not broken and vertical;
- the other leaves that are still in the top leafy cone have their insertion angle equally spaced between the vertical and the more external leaf in order to avoid any crossing between leaves;
- leaves that are fully developed and outside the top leafy cone are described using the model proposed by España [11].

### **2.1.2. Leaf senescence**

To get a realistic description of leaf senescence, we designed a simple algorithm based on the observation of the photographs of maize plants taken regularly during the growth season as described later in the model calibration section. Up to the anthesis, the first seven leaves have a particular developmental pattern [10, 17, 18]. Due to mechanical constraints imposed by stem growth and the associated decreasing light availability, these leaves separate from the stem, senesce, and finally fall. Observations show that during the early development phase there are never more than four leaves under the top leafy cone. When leaf eleven (7 + 4) is fully developed, the early senescence is stopped at the male anthesis.

### **2.1.4. Leaf dimensions and height**

A leaf is described by our model when it is visible at the top of the leafy cone, which is consistent with the definition of the leaf stage. In the top leafy cone, the insertion height of the leaves is considered as being that of the most external leaf of the top leafy cone. Leaf length is measured between the tip of the leaf and the insertion point. The width is the maximum width of the leaf.

Figure 1 shows that the leaf width is almost determined when the leaf emerges from the top leafy cone. It was therefore assumed to be constant and equal to the final value. Leaf height and length increase from leaf appearance up to their final values. We propose a unified approach for the description of its temporal evolution.

Let us consider the variable of interest  $x$ , that can be either leaf height or length. Because we always refer to the evolution of  $x$  up to its final (supposedly known) value, we will study the evolution of normalised value  $x^* = x/X$  where  $X$  is the final value of  $x$ . We then assume that  $x^*$  varies linearly with the leaf stage,  $\varphi$ , for each leaf order  $i$ :

$$x^*(\varphi, i) = 1 - a_x \cdot (\varphi_{1,x}(i) - \varphi) \quad (3)$$

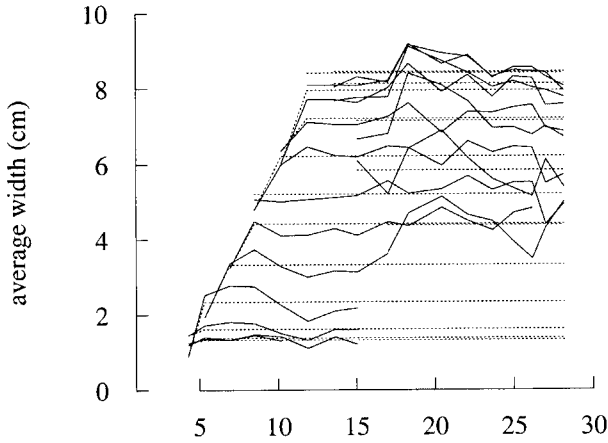


**Figure 1.** Measured width (solid lines) as a function of the leaf stage for the consecutive leaf order (1994 experimental field 1). The dotted lines correspond to the average final values.

where  $\varphi_{1,x}(i)$  is the leaf stage corresponding to the final value of  $x$  for leaf order  $i$ .  $a_x$  acts as an average growth rate and is considered independent of the leaf order.

The variable  $\varphi_{1,x}(i)$  may be approximated by a polynomial function of  $i$  for which the maximum is obtained for the last leaf order  $i_T$ .

$$\varphi_{1,x}(i) = a_x \cdot i^2 - 2 \cdot \alpha_x \cdot i_T \cdot i + \beta_x \quad (4)$$

For all leaf orders  $i$ , the normalised initial height and dimension  $x^*(i, i)$  are supposed to be greater than that of the first leaf,  $x^*(1, 1)$ . If we consider the leaf stage corresponding to leaf apparition, i.e. when  $\varphi = i$ , we get

$$x^*(i, i) = 1 - a_x \cdot (\varphi_{1,x}(i) - i) \geq x^*(1, 1) \quad (5)$$

Therefore,

$$(\varphi_{1,x}(i) - i) \geq \frac{1 - x^*(1, 1)}{a_x} \quad (6)$$

This equation is verified for all values of leaf orders  $i$ , if it is verified for the minimum of expression  $(\varphi_{1,x}(i) - i)$  which is obtained for:

$$i = i_T + \frac{1}{2 \cdot \alpha_x} \quad (7)$$

where  $i_T$  is the final number of leaves. Combining equations (4), (6) and (7) gives  $\beta_x$ :

$$\beta_x \geq \frac{1 - x^*(1, 1)}{a_x} + i_T + \alpha_x \cdot i_T^2 + \frac{1}{4 \cdot \alpha_x} \quad (8)$$

Considering equation (8), and (4) together gives:

$$\varphi_{1,x}(i) = \frac{1 - x^*(1, 1)}{a_x} + \alpha_x (i - i_T)^2 + i_T + \frac{1}{4 \cdot \alpha_x} \quad (9)$$

Equation (9) allows to estimate  $\varphi_{1,x}(i)$  for each leaf  $i$ , thus the normalised height and length as a function of the biological time (i.e. the leaf stage,  $\varphi$ ) if the parameters  $a_x$  and  $\alpha_x$  are known. The normalised values  $x^*(\varphi, i)$ , obtained from  $\varphi_{1,x}(i)$  and equation (3), can be multiplied by the final value  $X$  provided by the static model of the fully developed plant [11] to give the actual height or length of the leaf for any leaf order  $i$  at any time  $\varphi$  between emergence and male anthesis. In the next section, we will calibrate this dynamic model using a dedicated data set.

### 2.1.3. Stem diameter

The stem is represented by a truncated cone. The height of the stem corresponds to the insertion height of the last leaf, because we do not include the male flower. The dynamics of the insertion height of the leaves will be treated in the next section. According to España [11], the top  $r(i_T, \varphi_{1,h}(i_T))$  and bottom  $r(1, \varphi_{1,h}(i_T))$  radius of the fully developed plant stem verify:

$$r(1, i_T) = \gamma \cdot r(i_T, i_T) \quad (10)$$

with  $\gamma \approx 0.4$ . We assumed that the growth of the diameters of the truncated cone is proportional to the leaf stage  $\varphi$ :

$$r(i, \varphi) = \frac{\varphi}{\varphi_{1,h}(i_T)} \cdot r(i, \varphi_{1,h}(i_T)) \quad (11)$$

This simple model gives a realistic description of stem growth.

## 2.2. Calibration of the model

In this section, we will mainly focus on the leaf dimensions. The dynamic model has six parameters in addition to those of the static model:  $a_h$  and  $a_l$  act as an average growth rate,  $\alpha_h$  and  $\alpha_l$  correspond to the leaf appearance rate, and the normalised value  $h^*(1, 1)$  and  $l^*(1, 1)$  of the first leaf. These parameters will be calibrated over the data set.

### 2.2.1. The calibration data set

An experiment was carried out during summer 1994 at INRA's facility in Avignon (France). Two fields were sown with the same cultivar (DEA, France Maïs) with a month delay between both sowing dates. On each field, three samples of five plants were collected weekly. The measurements started from leaf 1 to male anthesis and included for all visible leaves:

leaf (laminae) insertion height, leaf length and maximum width. Leaf dimensions were measured according to the description in section 2.1.4. We additionally measured the top and bottom diameters of the stem. Further, the plants were photographed every week in front of a grid to archive their structure.

### 2.2.2. The calibration process

#### Insertion height

The  $a_h$  value was fitted on the normalised height values  $h^*(\phi, i)$  (figure 2a and 2b) using equation (3). It gives  $a_h = 0.177$ . Then, the leaf stage  $\phi$  corresponding to the final height for leaf order  $i$ ,  $\phi_{1,h}(i)$ , is fitted on the normalised height values  $h^*(\phi, i)$ . The parameter  $\alpha_h$  and the value  $h^*(1, 1)$  are finally adjusted using equation (9) and the values of  $\phi_{1,h}(i)$  computed previously. It gives  $\alpha_h = -0.072$  and  $h^*(1, 1) = 0.1$ . Figure 3a shows that the fit is very

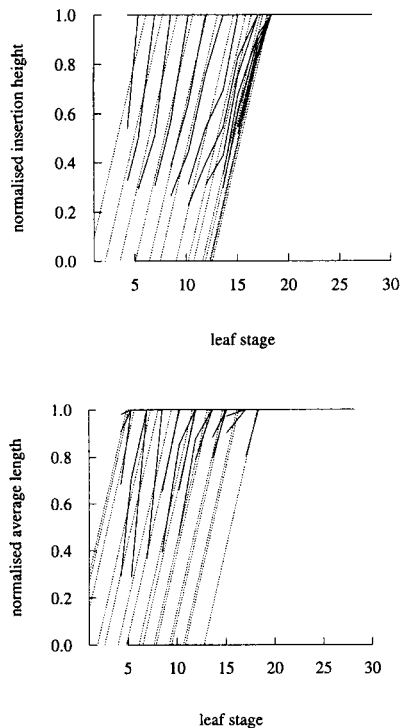


**Figure 2.** Normalised average leaf insertion height (a) and leaf length (b), as a function of the leaf stage, for the consecutive leaf order (1994 experimental field 1). The solid lines correspond to the measured values and the dotted lines to the model fit.

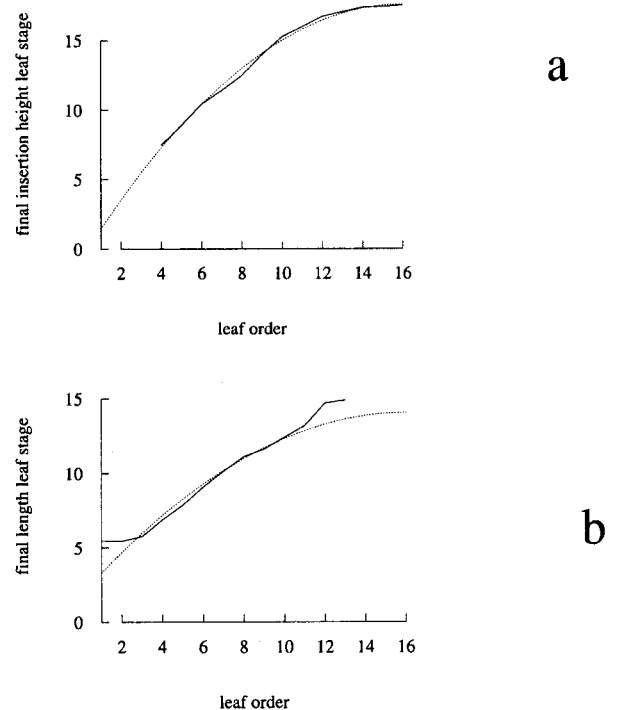


**Figure 3.** Leaf stage corresponding to the final leaf insertion height (a) and average final length (b), as a function of leaf order. The solid lines correspond to the experimental values and the dotted lines to the model fit.

good. Figure 4a shows the modelled normalised insertion height as compared to the measured values. The associated *RMSE* is 0.26, with  $R^2 = 0.83$  for the 67 data points available. The model has therefore relatively good performances, if we consider the experimental errors associated with the fact that at each date the plants sampled were different, and if we take into account the small number of parameters used in this model.

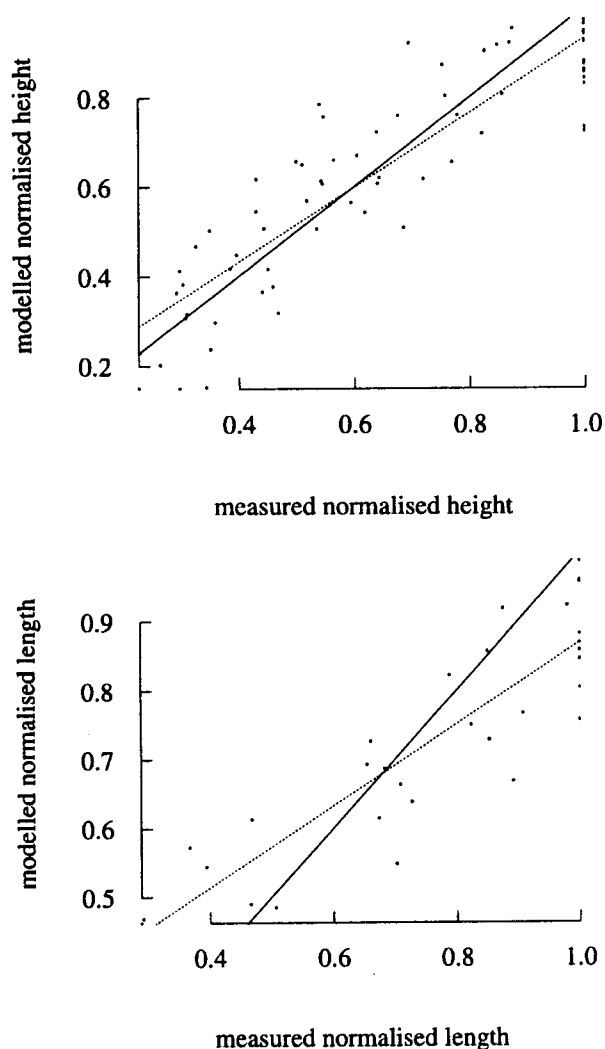


**Figure 4.** Comparison between measured and modelled leaf insertion heights (a) and leaf lengths (b) observed over 1994 experimental fields 1 and 2. The solid lines correspond to the 1:1 line and the dashed line to the best linear fit.

### Leaf length

Similarly to leaf insertion height, the average value of  $a_1$  is fitted over the data set and gives  $a_1 = 0.18$  (figure 2c and 2d). The leaf stage corresponding to the final leaf length,  $\phi_{1,i}(i)$ , is adjusted for each leaf order  $i$ . Finally, the quadratic relationship (equation (9)) between  $\phi_{1,i}(i)$  and  $i$  provides a good description (figure 3b) of the observations with adjusted parameters  $\alpha_i = -0.06$  and  $l^*(0) = 0.4$ . Figure 4b shows that the modelled normalised leaf length compares well to the measured values (*RMSE* = 0.23 and  $R^2 = 0.82$  for the 32 data points). The number of available data points for leaf length is lower than that of leaf height because leaf laminae length measurement of broken or disappeared leaves is not possible although their height can still be estimated because of the remaining sheath on the stem.

Figure 5 shows, as an example, a plant simulated by our 3D dynamic architecture model at different phenological stages.

## 3. MODEL VALIDATION

We acquired data sets corresponding to canopies different from those used to calibrate the model. Using the measured values of leaf area index, phenological stage, plant height and density, we generated 3D images of the corresponding stands. They were then visually compared with the actual canopies. Finally, further evaluation was performed, based on the comparison between measured and simulated gap fractions.

We will first describe the experiments used.

### 3.1. Experiments and measurements

#### 3.1.1. The experiments

We restricted the evaluation to the ability of the model to mimic the canopy architecture of a selection of crops grown under different conditions at



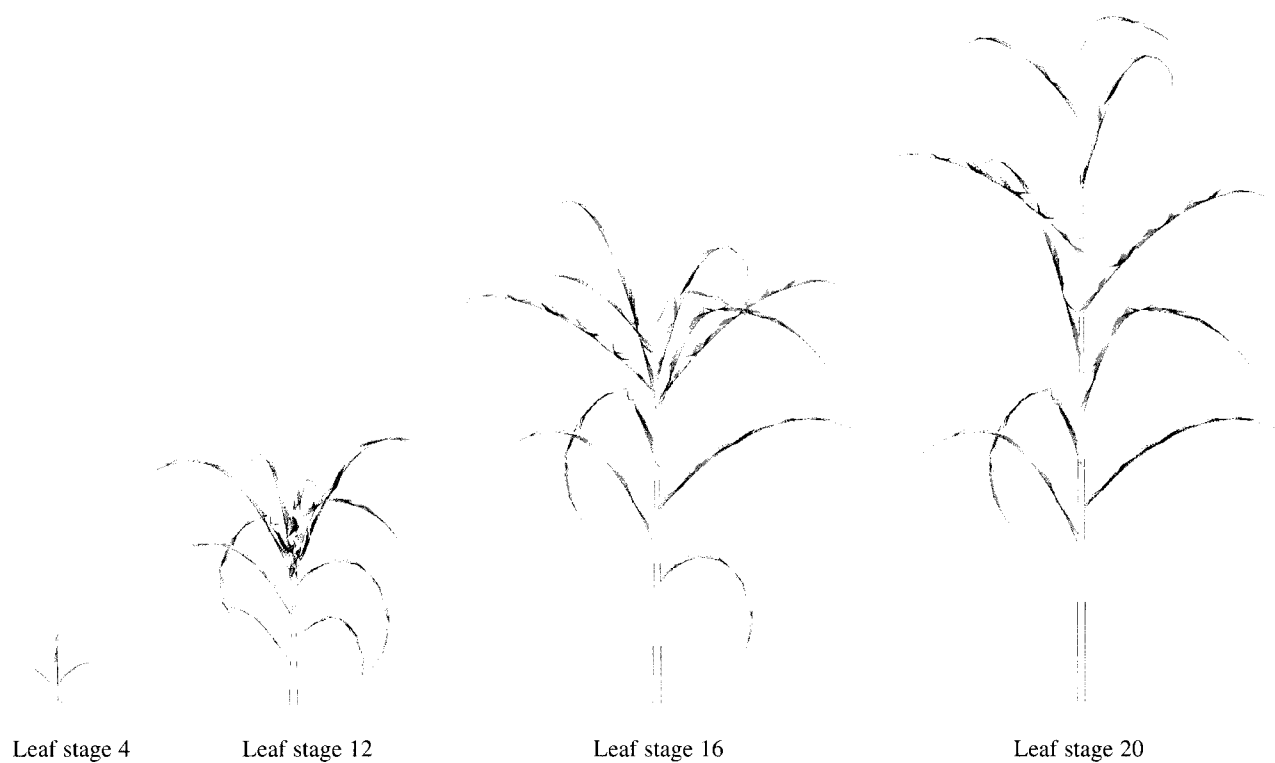


**Figure 5.** Example of a plant development simulated by the model (four-leaf stages)

specific phenological stages, rather than validating the model on a limited number of situations where the whole dynamics was measured. The growth conditions, the canopies used were subjected to for the validation process, were different (sowing date, density, year) from those which prevailed for the calibration process. Three experiments were used for the validation:

#### *INRA-90*

The experiment took place in 1990 at the INRA experimental facility in Avignon [3]. Two maize fields (cultivar: DEA, France Maïs) were sown at the same date but grown under two contrasted water status. The canopies were measured when the 14th leaf appeared. The plant density was 12 plant m<sup>-2</sup>.

#### *INRA-97*

The experiment took place in 1997 at the INRA experimental facility in Avignon (France) on a single maize field grown with the DEA cultivar. The measurements were performed at two phenological stages corresponding respectively to 13 and 17 visible leaves. The plant density was 8.5 plant m<sup>-2</sup>.

#### *Alpilles-97*

The experiment was part of the ReSeDA project [28] that took place in the Alpilles site, 30 km south of Avignon, during 1997. Three maize canopies, corresponding to the same cultivar (Cecilia, France Maïs), were sampled and had identical sowing date and plant density (7 plant m<sup>-2</sup>). They were grown in slightly different soil conditions and hence

expressed a corresponding variation in their vigour. Measurements were conducted when plants had about 15 visible leaves.

### 3.1.2. The measurements

Leaf area and plant height were measured during these experiments for the specific leaf stages considered. The leaf area index was estimated from the leaf area per plant and the plant density. The leaf area per plant was obtained, using a minimum of ten plants, from measurements of leaf length and width and multiplying the length and the width by an allometric coefficient of 0.73 [9, 21, 25]. Plant height was measured on the same samples.

Photographs were taken vertically for the days of the experiments to estimate the fraction cover [3]. The area sampled was approximately 3 m<sup>2</sup>.

For Avignon-90 and Avignon-97, a representative selection of plants were photographed over a grid to evaluate the realism of the simulations.

Table I shows the main characteristics of the canopies studied.

## 3.2. Generation of the simulated 3D canopies

Plants were described using the canopy model structure developed previously by España [11] cou-

pled with the dynamic model described in this study. The canopies were generated using the procedure proposed by España [11]. A small plot of 24 plants is repeated to infinity. Each leaf is represented using 20 triangles. España et al. [12] demonstrated that the radiative transfer was only marginally affected by this degradation of canopy structure representation.

The input variables of the 3D dynamic architecture model are the leaf stage, the plant density, the leaf area cumulated over the fully developed plant including the leaves that senesced, and the final height of the canopy. As plant development was not completed at the time of the experiments, we did not have a measure of the cumulated leaf area, nor the final plant height. Therefore, these two variables were adjusted so that the simulated leaf area index and plant height agree with the field observations at the time of the measurement. The balance between these two variables in the adjustment process was mainly governed by the realism of the early stages of leaf appearance within the top leafy cone. The input variables appear in table II.

## 3.3. Evaluation of the 3D dynamic architecture model

The evaluation of the 3D dynamic architecture model will be achieved using three criteria:

**Table I.** Characteristics observed for the crops used in the model validation process.

	Treatment	Cultivar	Plant density (plants m <sup>-2</sup> )	Leaf stage	Plant height (m)	LAI	Cover fraction
INRA-90	1	DEA	12	10	0.30	0.44	0.13
	2	DEA	12	10	0.47	1.0	0.35
INRA-97	1	DEA	8.5	13	0.45	3.0	—
	2	DEA	8.5	17.8	1.70	4.5	0.87
Alpilles-97	1		7	15.4	0.70	2.34	0.33
	2		7	15.4	0.90	2.86	0.44
	3		7	15.4	1.10	3.26	0.47

**Table II.** Variables (cumulated leaf area, final height and number of leaves) of the fully developed plant 3D architecture model adjusted to fit the observations at given leaf stages for the validation cases. The extinction coefficient used in equation (1) for nadir viewing ( $K(\theta)$ ) are also indicated. They are either derived from the cover fraction and leaf area index measurements, or from the simulated 3D canopies.

	Treatment	Cumulated leaf area (m <sup>2</sup> )	Final height (m)	Number of leaves	$K(\theta)$ Experimental	$K(\theta)$ 3D model
INRA-90	1	0.18	2.2	19–22	0.31	0.34
	2	0.24	2.4	21–23	0.43	0.37
INRA-97	1	0.6	1.9	19	–	0.33
	2	0.6	3.0	19	0.45	0.27
Alpilles-97	1	0.34	2.0	17	0.17	0.29
	2	0.41	3.0	17	0.20	0.30
	3	0.44	3.6	17	0.20	0.27

- the realism of the adjusted values of the cumulated leaf area index and final plant height;
- the visual comparison between the generated and the actual plants and canopies;
- the comparison between the simulated and the measured cover fraction.

### 3.3.1. Realism of the adjusted input variables

The adjusted values of the final number of leaves were constrained within a known range of variation. The adjusted values of cumulated leaf area, and final plant height appear not to always be realistic, even if they remain in the possible range of values (table II). For example, the two phenological stages of INRA-97 were generated with two different values of plant height in order to better mimic the actual leafy cone aspect. It appears to be difficult to model accurately the top leafy cone dynamics, because it develops very fast.

### 3.3.2. Visual comparison between actual and simulated plants and canopies

The distribution of the parameters and variables describing leaf shape and curvature, such as the number and the position of broken leaves or the leaf insertion angle, has been adapted to better represent

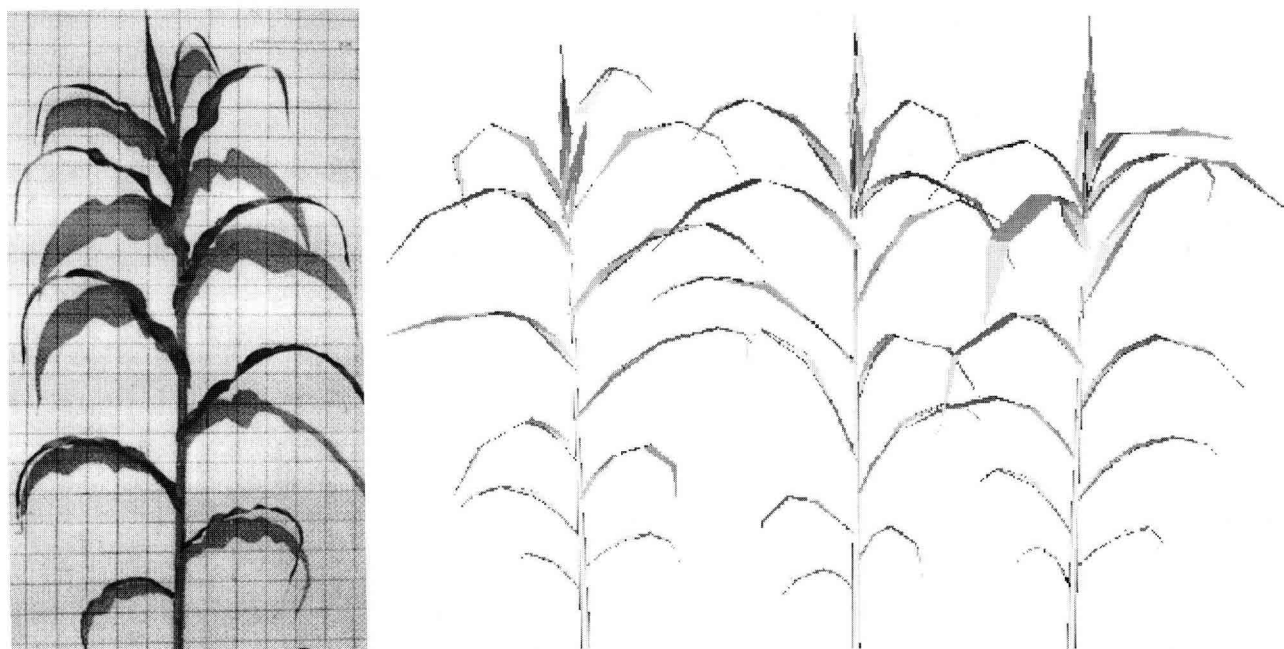
the observed plant silhouettes. This was mainly driven by the realism of the leafy cone, corresponding to not-fully expanded leaves.

Figure 6 shows an example of the comparison between actual silhouette photographs and the silhouette of plants generated by the model. The simulation gives a quite realistic plant architecture. Nevertheless, slight differences were noticed in actual leaf lengths, particularly for INRA-97 experiment.

Plant azimuth rotation, described as being random in España [11], has been modified when necessary to better simulate the actual plant arrangement. This was the case when plants were in the latest development stages, as in the second date of the INRA-97 experiment, for which leaves were nearly perpendicular to the rows (figure 7). Literature review shows contradictory observations on leaf possible re-orientation. Girardin [16] and Girardin and Tollenaar [17, 18] reported a leaf azimuth re-orientation perpendicular to rows, independently to its initial position. Conversely Drouet and Moulia [8] do not observe such leaf re-orientation.

### 3.3.3. Comparison between the simulated and the actual cover fraction

Estimation of the cover fraction is achieved by projecting the area of the elementary triangles that



**Figure 6.** Actual silhouette photograph of a plant (leaf stage 17) compared to plants simulated by our model.



**Figure 7.** Nadir looking photograph of the INRA-97 canopy for the second date (17 leaves).

compose the computerised canopy onto a plan perpendicular to the observation direction. The cover fraction corresponds to the complement to unity of the nadir gap fraction. Results (*figure 8*) show a general good agreement between the cover fraction measured from vertical photographs and the cover fraction estimated by projection ( $R^2 = 0.72$ ;  $RMSE = 0.12$ ). Part of the scattering observed can be attributed to the relatively small area sampled by the photographs for the estimation of the cover fraction.

The extinction coefficient  $K(\theta)$  used in equation (1) computed for nadir using the 3D architecture model is in the range 0.27–0.37 with an average value of  $K(\theta) = 0.30$  (*figure 9*). This is in good agreement with the results of Andrieu et al. [2] who measured an average value of 0.34. The experimental values of the extinction coefficient derived from the photographs taken in the fields are more scattered, in the range 0.17–0.45, presumably due to errors both in the evaluation of the leaf area index and in the gap fraction (or cover fraction). The extinction coefficient computed from the 3D dynamic model appears not to be very sensitive to the development stage or the leaf area index (*figure 9*). The increase in leaf overlap between consecutive plants when the canopy grows is presum-

ably partly compensated by leaf azimuth rotation mechanisms that decrease canopy clumpiness.

These results show that the 3D dynamic canopy architecture model provides a relatively accurate description of the actual canopy structure. The model can therefore be used to analyse in greater details the clumping of the canopy, both as a function of the phenological stage and the direction of the observation.

#### 4. APPLICATION TO THE DESCRIPTION OF THE CLUMPINESS OF MAIZE CANOPIES

As discussed in the introduction, the clumpiness of the canopy is generally described by the clumping parameter  $\lambda_0$ . We will make here various assumptions about its possible factors of variation, and evaluate their respective performances for the description of the directional gap fraction. This will be done using our 3D dynamic model to generate a temporal series of maize canopy structure. The corresponding directional gap fraction is computed for each canopy using the same projection technique as in section 3.3.3. Andrieu and Sinoquet [1] showed

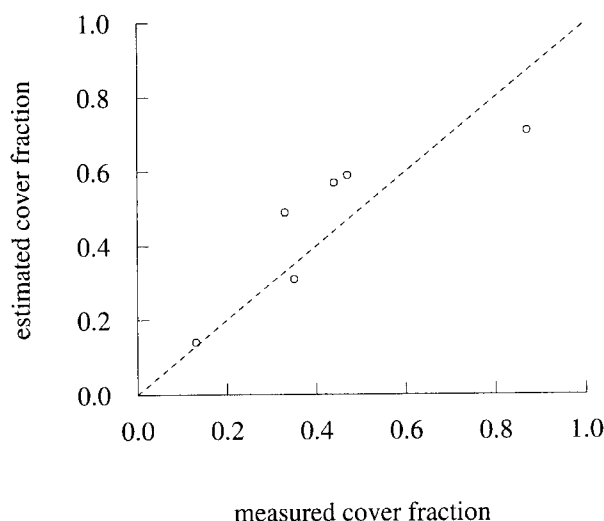


**Figure 8.** Comparison between the measured cover fraction and that estimated on the corresponding 3D architecture model. The dashed line is the 1:1 line.

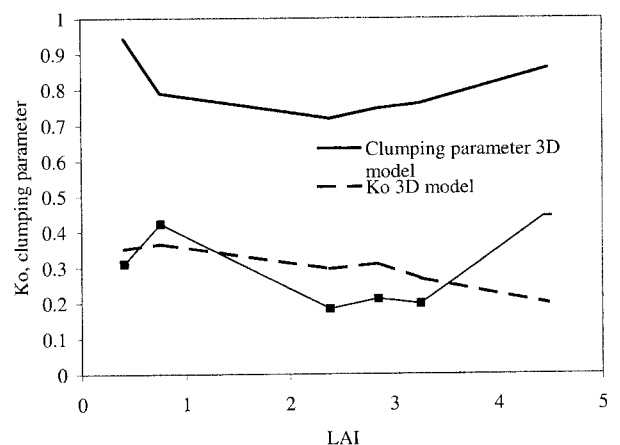


**Figure 9.** Extinction coefficient ( $K(\theta)$ ) and clumping parameter as a function of the leaf area index.

that the gap fraction is not very sensitive to the azimuth of the row, except in situations where the direction of the observation is parallel to that of the row. We therefore restricted the study to a 45° azimuth observation angle from the row direction. The clumping parameter is then adjusted on the computed directional gap fractions using equations (1) and (2).

#### 4.1. The canopies simulated

The canopies simulated are made of three rows of 8 plants. The rows are spaced by 0.7 m and the distance between plants is 0.2 m, leading to a plant density of 7.14 plant m<sup>-2</sup>. This elementary patch is replicated to infinity in order to simulate a large maize field and avoid border effects in the gap fraction computation. A previous study [12] showed that 24 plants allow a good representation of an homogeneous field.

The canopies simulated correspond to 6 leaf stages of the same maize crop. The plants were generated using distribution laws of the model input variables. The distribution laws were those observed in the calibration experiment with average values of 0.47 m<sup>2</sup> for the cumulated plant leaf area, 1.80 m for the final height and 16 to 19 leaves for the final number of leaves.

The six phenological stages were chosen to get a good sampling of the leaf area seasonal development (table III).

#### 4.2. Variability of the clumping parameter

We will test here four assumptions on the factors of variation of the clumping parameter  $\lambda_0$ . They are used to constrain the fit between the theoretical gap fraction model described by equations (1) and (2) and the gap fraction derived by projection techniques applied to the 3D architecture model. The leaf inclination distribution function used was that derived from the 3D architecture model. The clumping parameter, when adjusted, is fitted over the directional gap fraction values using equations (1) and (2) and the LAI value. Table IV presents the four assumptions used and the associated performances.

##### Assumption 1

The canopy is assumed to be made up of infinitely small leaves randomly distributed positionally. The clumping parameter is set at 1.0. Figure 10a shows that the gap fraction is not very accurately described. A systematic overestimation is observed, because the clumpiness of the canopy was not accounted for.

##### Assumption 2

The clumping parameter is assumed to depend only on the observation direction  $\theta$ , and not on the phenological stage. The  $\lambda_0$  parameter was thus adjusted for each observation over the whole set of

**Table III.** Characteristics of the six-leaf stages simulated in the sensitivity analysis.

Phenological Stage	Leaf stage	Leaf area index	Plant height (m)	Cover fraction	Average leaf inclination (°)
1	4	0.26	0.09	0.07	56
2	8	0.88	0.20	0.20	63
3	12	1.70	0.41	0.36	59
4	16	2.50	0.82	0.48	58
5	18	3.36	1.70	0.60	52
6	24	3.40	1.80	0.6	53

phenological stages. The  $\lambda_0$  as a function of the observation angle (figure 11a) shows that the canopy is more clumped for nadir directions, presumably because of the row effect. For  $30^\circ$  observation angle, the clumping parameter reaches a maximum, close to 0.8, indicating a more random dispersion of leaves. For larger zenith angles, the apparent clumping increases, which might result from a lack of sensitivity of the gap fraction occurring when the optical path increases. The difference between the fitted and actual values of the gap fraction as a function of the observation angle (figure 10b) shows some error pattern for the latest phenological stages.

### Assumption 3

The clumping parameter is assumed to depend only on the phenological stage, and not on the observation direction. It was therefore adjusted for each phenological stages over the whole set of observation angles. Figure 11b shows that the clumping parameter is higher for the youngest canopies corresponding to the lowest leaf area indices. This indicates less clumpiness, partly explained by the regular sowing pattern that reduces the overlap between small plants. At the intermediate stages, the presence of the leafy cone, where leaves are quite vertical and clumped together, explains the increase in canopy clumpiness. For the

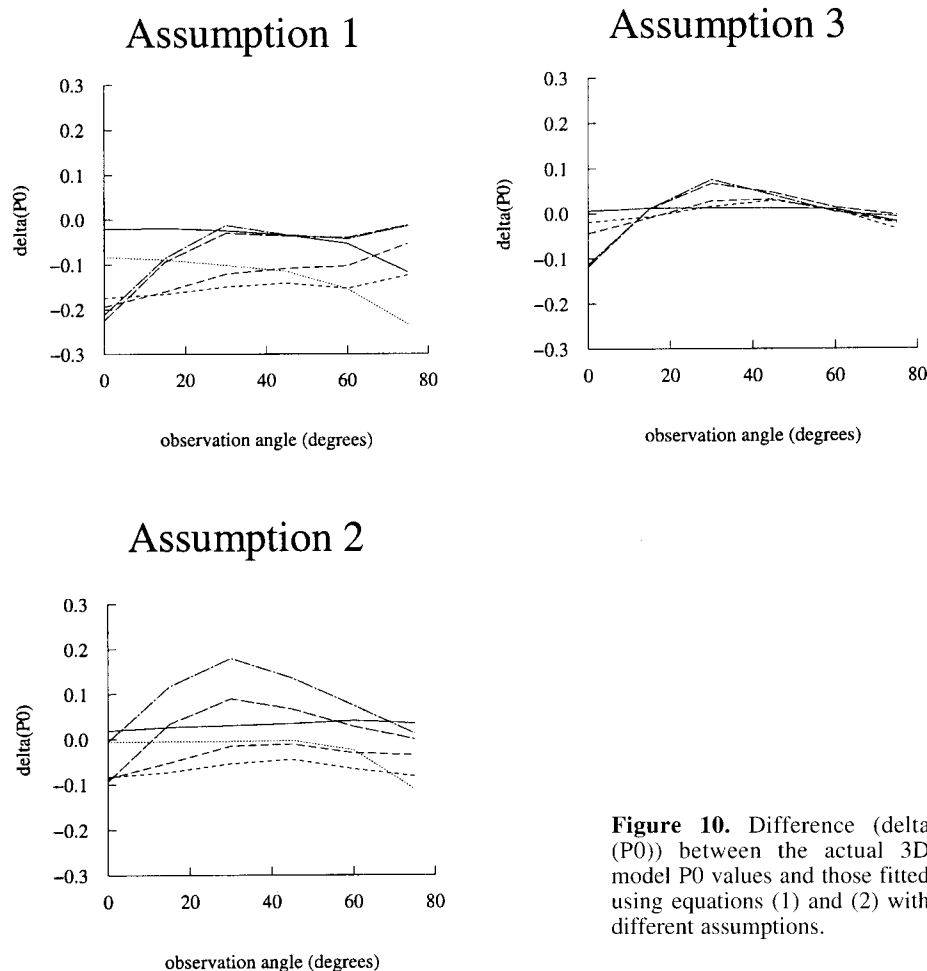


**Figure 10.** Difference ( $\delta(P_0)$ ) between the actual 3D model  $P_0$  values and those fitted using equations (1) and (2) with different assumptions.

oldest well developed canopies, the slight decrease of canopy clumpiness is probably due to the disappearance of the leafy cone. Comparison between fitted and actual values for the gap fraction shows (figure 10c) that the error are significantly smaller than that of assumption 2. However, some directional error pattern is observed for the last two stages corresponding to the higher leaf area index values.

#### Assumption 4

The clumping parameter, is assumed to depend both on the phenological stage and on the observation direction. It was adjusted for each phenological stage and each observation direction. It can be cal-

culated analytically using equations (1) and (2) and leads obviously to a perfect fit for the gap fraction. The  $\lambda_0$  as a function of the observation angle and leaf area index (figure 11c) confirms the results found for assumptions 2 and 3. The youngest and oldest canopies have a more clumped character than intermediate stages. For all phenological stages, clumpiness is more important for near-nadir directions and for fully-developed plants, where the row effect is at a maximum. The apparent increase of clumpiness for the more oblique directions and the highest leaf area indices might result from a lack of sensitivity of the gap fraction occurring when the optical path increases, similarly to what was observed for assumption 2.

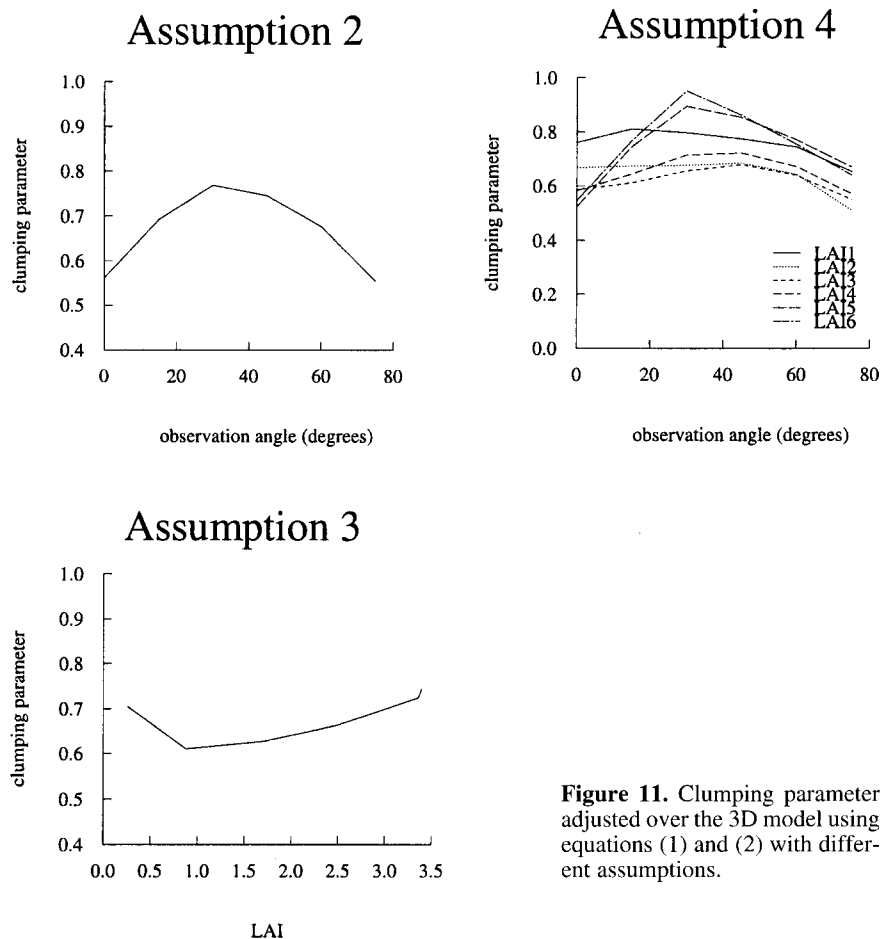


**Figure 11.** Clumping parameter adjusted over the 3D model using equations (1) and (2) with different assumptions.



**Table IV.** The four assumptions tested and the corresponding RMSE evaluated on the directional gap fraction for the six-leaf stages considered.

Assumption	Clumping parameter $\lambda_0$	RMSE observed on the directional gap fraction
1	$\lambda_0 = 1.0$	0.11
2	$\lambda_0$ depends only on the direction $\theta$	0.07
3	$\lambda_0$ depends only on the phenology	0.04
4	$\lambda_0$ depends on the phenology and on the direction $\theta$	0.00 (perfect fit by construction)

## 5. CONCLUSION

One of the main objective of this work was to develop a 3D dynamic architecture model of maize canopies for accurate simulation of the radiative transfer, both for canopy functioning and for remote sensing applications. Therefore, the approach used was mainly driven by the possibility of simulating a wide range of situations with the following input variables:

- the canopy sowing pattern (row spacing and orientation, plant spacing), which is generally fixed for given climatic conditions and cultivars;
- the final number of leaves produced by the plant, which is mainly driven by its genetic potential, and the final plant height which depends on the genetic potential of the plants, the pedo-climatic conditions as well as plant density;
- the cumulated plant leaf area, which also depends on the same set of factors.

The time is described by the leaf stage which can easily be translated into cumulated growth degree days values.

The 3D dynamic model developed here describes the temporal growth of maize canopies architecture with this relatively limited number of input variables, while giving globally good performances, as showed by the evaluation performed with an independent data set. However, we noticed problems in the simulation of the top leafy cone, which is quite difficult to describe because it corresponds to the synchronisation of a series of rapid growth process-

es occurring at the stem level, and at the level of the sheath and laminae of several leaves. Another important still unsolved question regards the possible re-orientation of leaves. The description of leaf curvature is based on rules derived from few observations without distinguishing leaf order and plant development stage. Further studies should investigate in more details this aspect, particularly for canopies subjected to water stress, and when considering different cultivars. Finally, the current model does not address post-anthesis development phase, mainly characterised by leaf senescence.

The validation of the model is limited because of the size of the data sets used and because they do not cover the whole growth season. Therefore, additional validation of the model is required, either directly on canopy structure variables, or preferably, on variables of interest such as the gap fraction, the fraction of photosynthetically active radiation absorbed by the canopy, or on the bi-directional reflectance.

In the second part of this study, we applied our 3D dynamic architecture model to the investigation of ways to simply describe the canopy gap fraction. We demonstrated that maize canopies have a marked clumped character. It is therefore necessary to use a clumping parameter in the classical exponential function (equation (1)) to account for the non-random arrangement of leaves within the canopy. The directional behaviour of the clumping parameter is significant for the oldest phenological stages corresponding to the higher leaf area indices, and for observation close to the nadir. This is pre-

sumably explained by the row character of the canopy. The gap fraction is better described when the clumping parameter is a function of the development of the canopy and the observation angle. The question which arises concerns the choice of the variable that better represents canopy development. We assumed in this study that it was mainly driven by the phenological stage. However, it could also be driven by the leaf area index of the canopy. Further studies are needed to address this issue.

The degree of accuracy of a model should always be consistent with what the model is to be used for. That is the reason why, even with the possible imperfect representation of the actual canopy structure by the model, sensitivity analysis of the model should be conducted in order to evaluate the proper degree of accuracy required for adequate simulation of the variables of interest such as the gap fraction, the fraction of absorbed photosynthetically active radiation, or the bi-directional reflectance. Iteration between model improvement, sensitivity analysis and model validation should lead to a quite comprehensive approach. The present study therefore appears as the first step of this iterative process.

## REFERENCES

- [1] Andrieu B., Sinoquet H., Evaluation of structure description requirements for predicting gap fraction of vegetation canopies, *Agric. For. Meteorol.* 65 (1993) 207–227.
- [2] Andrieu B., Allirand J.M., Jaggard K., Ground cover and leaf area index of maize and sugar beet crops, *Agronomie* 17 (1997) 315–321.
- [3] Baret F., Experiment III, Montfavet, France, July–August 1990. Report and Data., Institut national de la recherche agronomique, station de bioclimatologie, Montfavet, France, 1992.
- [4] Baret F., Andrieu B., Steven M.D., Gap frequency and canopy architecture of sugar beet and beet crops, *Agric. For. Meteorol.* 65 (1993) 261–279.
- [5] Chen S.G., Impens I., Ceulemans R., Kockelbergh, Measurement of gap fraction of fractal generated canopies using digitalized image analysis, *Agric. For. Meteorol.* 64 (1993) 245–259.
- [6] Chen S.G., Ceulemans R., Impens I., A fractal-based *Populus* canopy structure model for the calculation of light interception, *For. Ecol. Manage.* 69 (1994) 97–110.
- [7] Colheo D.T., Dale R.F., An energy-crop growth variable and temperature function for predicting corn growth and development: Planting to silking, *Agron. J.* 72 (1980) 503–510.
- [8] Drouet J.L., Moulia B., Ré-orientations spatiales des feuilles de maïs au cours de la croissance végétative en fonction de l'orientation initiale et de la densité des plantes, Actes du séminaire sur la modélisation architecturale, Paris, Inra, 1997, pp. 153–158.
- [9] Dwyer L.M., Stewart D.W., Leaf area development in field-grown maize, *Agron. J.* 78 (1986) 334–343.
- [10] Duburcq J.B., Bonhomme R., Derieux M., Durée des phases végétative et reproductive chez le maïs, *Agronomie* 3 (10) (1983) 941–946.
- [11] España M.L., Simulation de la variation temporelle, directionnelle et spectrale de la réflectance de cultures de maïs à partir d'un modèle dynamique de la structure 3D du couvert, Ph.D. thesis, Marne-la-Vallée University, France, 1997, 239 p.
- [12] España M.L., Baret F., Chelle M., Aries F., Andrieu B., Modélisation 3D du maïs pour la simulation de la réflectance, Actes du séminaire sur la modélisation architecturale, Paris, Inra, 1997, pp. 89–98.
- [13] Fournier C., Andrieu B., A 3D architectural and process-based model of maize development, *Ann. Bot.* 81 (1998) 233–250.
- [14] Fournier C., Andrieu B., Utilisation de l'approche L-système pour la modélisation architecturale du développement du maïs, Actes du séminaire sur la modélisation architecturale, Paris, Inra, 1997, pp. 203–212.
- [15] Girardin Ph., Morel-Fourrier B., Jordan M.O., Millet B., Développement des racines adventives chez le maïs, *Agronomie* 7 (5) (1987) 353–360.
- [16] Girardin Ph., Leaf azimuth in maize canopies, *Eur. J. Agron* 1 (2) (1992) 91–97.
- [17] Girardin Ph., Tollenaar M., Leaf azimuth in maize: origin and effect on canopy patterns, *Eur. J. Agron.* 1 (4) (1992) 227–233.
- [18] Girardin Ph., Tollenaar M., Effects of intraspecific interference on maize leaf azimuth, *Crop Sci.* 34 (1994) 151–155.

- [19] Goel N.S., Knox L., Norman J., From artificial life to real life: Computer simulation of plant growth, *Int. J. Gen. Syst.* 18 (1991) 291–319.
- [20] Jaeger M., de Reffie P., Basic concepts of computer simulation of plant growth, *J. Biosci.* 17 (3) (1992) 275–291.
- [21] Keating B.A., Wafula B.M., Modelling the fully expanded area of maize leaves, *Field Corn Res.* 29 (1992) 136–176.
- [22] Kuusk A., A Markov chain canopy reflectance model, *Agric. For. Meteorol.* 6 (1995) 221–236.
- [23] Lewis P., The Botanical Plant Modelling System (BPMS), *Actes du séminaire sur la modélisation architecturale*, Paris, Inra, 1997, pp. 45–53.
- [24] Lewis P., Muller J.P., Botanical plant modelling system for remote sensing simulation studies, *Proc. Int. Geosci. Remote Sens. Symp.*, Washington DC, USA, May 21–24, 1990, pp. 1739–1742.
- [25] McKee G.W., A coefficient for computing leaf area in hybrid corn, *Agron. J.* 56 (1964) 240–241.
- [26] Nilson T., A theoretical analysis of the frequency of gaps in plant stands, *Agri. Meteorol.* 8 (1971) 25–38.
- [27] Myneni R.B., Ross J., Asrar G., A review on the theory of photon transport in leaf canopies, *Agric. For. Meteorol.* 45 (1989) 1–151.
- [28] Prévot L., Assimilation of Multi-Sensor and Multi-Temporal Remote Sensing Data to Monitor Vegetation and Soil: the Alpilles-ReSeDA project, *Proc. Int. Geosci. Remote Sens. Symp.*, Seattle, WA, USA, 1998.
- [29] Prusinkiewicz P., A look at the visual modeling of plants using L-systems, *Actes du séminaire sur la modélisation architecturale*, Paris, Inra, 1997, pp. 55–70.
- [30] Prusinkiewicz P., Lindenmayer A., *The Algorithmic Beauty of Plants*, Springer-Verlag, New York, 1990.
- [31] de Reffye Ph., Edelin C., Françon J., Jaeger M., Puech C., Plants models faithful to botanical structure and development, *Comput. Graphics* 22 (4) (1988) 151–158.
- [32] de Reffye P., Houllier F., Blaise F., Barthélémy D., Dauzat J., Auclair D., A model simulating above- and below-ground tree architecture with agroforestry applications, *Agrofor. Syst.* 30 (1995) 175–197.
- [33] Ross J., Radiative transfer in plant communities, in: Monteith J.L. (Ed.), *Vegetation and the Atmosphere*, vol.1, Academic Press, London, 1975, pp. 13–52.
- [34] Warrington I.J., Kanemasu E.T., Corn growth response to temperature and photoperiod. I. Seeding emergence, tassel initiation, and anthesis, *Agron. J.* 53 (1983) 749–754.
- [35] Warrington I.J., Kanemasu E.T., Corn growth response to temperature and photoperiod. I. Leaf-initiation and leaf-appearance rates, *Agron. J.* 53 (1983) 755–761.
- [36] Warrington I.J., Kanemasu E.T., Corn growth response to temperature and photoperiod II. Leaf number, *Agron. J.* 53 (1983) 762–766.